ISSN(Online): 2319-8753
ISSN (Print): 2347-6710

International Journal of Innovative Research in Science, Engineering and Technology

(An ISO 3297: 2007 Certified Organization)

Vol. 5, Issue 6, June 2016

Crash Analysis of Unmanned Aerial Vehicle Using FEA

Mahantayya KHiremath[1], Somashekar V [2]

Assistant Professor, Department of Aeronautical Engineering, Acharya Institute of Technology, Bangalore, India[1]

Assistant Professor, Department of Aeronautical Engineering, Acharya Institute of Technology, Bangalore, India[2]

ABSTRACT:Even though there are lots of technology advancements in the field of Unmanned Aerial Vehicle (UAV), there is high possibility that an aerial vehicle will crash during initial test trials and in subsequent flights and hence loss high cost equipment's along with loss of airplane structural components and money invested on it. Main interest in the present work is to analyse the possible accidents that designed UAV goes through and find out the peak impact forces at the important locations in the UAV where most of the electronic equipment's are installed. In any crash we cannot avoid damage to the structure. So even after the crash we should not lose the data which is acquired during the surveillance, terrain mapping, reconnaissance, in this work our aim is to extract the peak impact (nodal dynamic forces) at Main electronic equipment's like surveillance camera, servomotors, fuel tank, payload, receiver etc.After crash no structure is safe but the costlier components like surveillance camera, servomotors, fuel tank, payload, receiver etc. can be reused to rebuild UAV within less time and can be made ready for successive flight with no much difficulty in design and construction.

KEYWORDS: Crash Analysis, UAV, Structural Analysis, Nose Landing, Belly Landing

I. INTRODUCTION

A lot of research was made throughout the years but unfortunately, there was not a single prototype capable of completing the job required with 100% accuracy. It was not until late 1980s and early 1990s that the technology started to catch up with this idea of radio control airplanes. At that time, a new term was created for those devices; it was the start of the Unmanned Aerial Vehicles (UAV) era. Due to the great advantages of having a Plane being controlled by remote and not by a person, Several countries started to invest more and more in this idea until it became what it is today. Thanks to the advances in the radio control technology, the armed forces have been able to save many soldier's lives by using the radio controlled or UAVs airplanes instead of an aircraft piloted by a human. Now-a-days UAVs are used extensively by several defence forces for surveillance, reconnaissance and terrain mapping purposes.

The main objective of the present work is to analyse the possible accidents that a designed UAV goes through, and find out the peak impact forces at important locations in the UAV where most of the electronic equipment's are installed. Data which is acquired during the surveillance, terrain mapping, and reconnaissance are not to be lost. In this work, our aim is to extract the peak impact (nodal dynamic forces) of Main electronic equipment's like surveillance camera, servomotors, fuel tank, payload, receiver etc. After crash no structure is safe but the costlier components like surveillance camera, servomotors, fuel tank, payload, receiver etc., can be reused to rebuild UAV within less time and can be made ready for successive flight with not much difficulty in design and construction.
The peak dynamic forces from UAV crash study in LS DYNA are taken into consideration of the design of the box structure which supports for various components installed in the nose section as well as in the centre fuselage section of UAV for future scope of optimization of box structure.

The below Table 1 shows the in detail materials required for the construction of UAV and with section properties are mentioned and also these materials are defined for the LS Dyna solver as per its material models.

ISSN(Online): 2319-8753
ISSN (Print): 2347-6710

International Journal of Innovative Research in Science, Engineering and Technology

(An ISO 3297: 2007 Certified Organization)

Vol. 5, Issue 6, June 2016

Sl. No.	Components	Materials	LS-Dyna Material model	Section Properties
1	Front Nose	Balsa wood	MAT 54/55	5mm thick
2	Mass support	Aluminum	MAT 24	4mm thick
3	Wing skin	Balsa wood	MAT 54/55	1.6mm thick
4	Wing ribs	Balsa wood	MAT 54/55	3mm thick
5	Nose attachment	Balsa wood	MAT 54/55	10mm thick
6	Cage	Balsa wood	MAT 54/55	5mm thick
7	Cage attachment	Balsa wood	MAT 54/55	5mm thick
8	Tail Connections	Balsa wood	MAT 54/55	5mm thick
9	Landing gear	Steel	MAT 1	6.35mm thick
10	Mid ribs	Aluminum	MAT 24	17mm dia
11	Front wing spar1	Carbon fibre	MAT 3	15.87mm dia
12	Front wing spar2	Carbon fibre	MAT 3	9.53mm dia
13	Connecting rod	Carbon fibre	MAT 3	17mm dia
14	Rear wing spar	Aluminum	MAT 24	9.53mm dia

Table 1: Materials and materials properties

II. METHODOLOGY

2.1. Modeling of UAV: It is known that preparation of the geometric model to any analysis is the crucial part of the initial stages of the work and the model is referred from one of the main reference [2], the most prominent CAD software for modeling complicated surface structures is CATIA V5. Hence in this present work CATIA V5 is used to develop the initial geometry required for analysis with nearest accuracy to that of the ref [2].

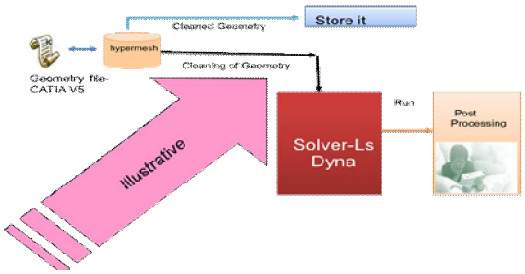

Fig 1: Methodology

2.2. FE Modeling of UAV: Once after preparation of the geometric model, next process in this study is to prepare finite element model of the UAV. In this work it is very difficult to clean up the geometry because some of the curves, surfaces or some other data can be lost while transferring model from any CAD software to FEA software. Hence for any pre-processor, it is important to do geometric clean-up where some of the missing curves or surfaces or some extra features are corrected for geometric accuracy.

ISSN(Online): 2319-8753
ISSN (Print): 2347-6710

International Journal of Innovative Research in Science, Engineering and Technology

(An ISO 3297: 2007 Certified Organization)

Vol. 5, Issue 6, June 2016

2.3. Solver Tool for Crash of UAV: In the present work, LS-DYNA is the chosen software and Crash analysis of a UAV has been carried out for two different configurations. LS-DYNA uses proven explicit time integration technique to solve the nonlinear dynamic response analysis problem. It contains a complete library of finite elements (type/shapes/orders) and numerous material models to simulate the nonlinear behaviour of materials.

2.3.1 Basics of Non-linear Analysis

This section reviews nonlinear structural problems by looking at the event and the physical sources of nonlinear behaviour. The finite element method (FEM), or finite element analysis (FEA), is based on the idea of building a complicated object with simple blocks or dividing a complicated object into small and manageable pieces (elements and nodes). In the **Figure 2a** is shown a plate with a hole subjected to a compression load and its FEM discretisation is shown in Figure 2b.

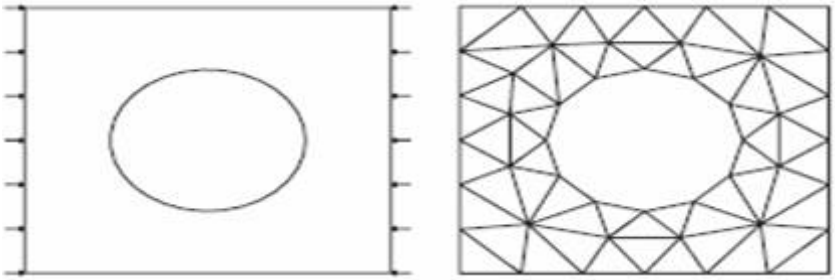

Fig 2a: Plate with hole**Fig 2b:** FE model

The finite element method (FEM) consists of the following five steps:

1. **Pre-processing**: subdividing the problem domain into finite elements.
2. **Element formulation**: development of equations for elements.
3. **Assembly**: obtaining the equations of the entire system from the equations of individual elements.
4. **Solving the equations**.
5. **Post processing**: determining quantities of interest, such as stresses and strains, and obtaining visualizations of the response.

The fundamental FEA equation is:

$$Ku_e = F \qquad (1)$$

Where K is the stiffness matrix, $u_e$the element displacements and F the applied loads. The solution of the equation is usually straightforward and can be reached in a single step by applying **F**, inverting **K**. Furthermore it is possible to go back and determine the stress (**σ**)and the strain. Nonlinear structural analysis is the prediction of the response of nonlinear structures by model-based simulations, like Finite Element Analysis and the relative equations are usually solved by incremental methods, such as the implicit or explicit methods.

Nonlinearities can rise for many reasons. For structural analysis there are four sources of nonlinear behaviour and the corresponding nonlinear effects are identified by the terms material, geometric, force B.C. and displacement B.C., in which B.C. means ”Boundary Conditions” In the following subsections these sources of nonlinearities are correlated to the physics in more detail.

III. MODELING

3.1 Development of Geometrical Model

As the design process is the most important part in the project and it is a tedious job to deal with, since the model which we are interested is not of a single component. It is an assembly of many subcomponents. Hence all the components are modeled and assembled based on the data available [2]. So the first step in modeling starts with historical data of airfoil and wing span and its arrangement in the assembly. So the airfoil chosen for the main wing structure are CH10 at root

ISSN(Online): 2319-8753
ISSN (Print): 2347-6710

International Journal of Innovative Research in Science, Engineering and Technology

(An ISO 3297: 2007 Certified Organization)

Vol. 5, Issue 6, June 2016

and FX63-137 at the tip [2]. Since CATIA V5 is a hi-end CAD tool for designing and drafting, in this present work CATIA V5 is used for geometrical modeling. Initially the airfoil data from excel is imported to CATIA windows via Macros and the required shape of airfoil has been created and the scaled to chord length at each section of span is shown below. Likewise all the components are modeled as per dimensions available in reference [2].

Maximum dimensions in (mm)		
L	Maximum length	1614.27
H	Maximum height	578.52
B	Wing span	2622.8
B	Tail span	505
Dimensions total (mm)		5320.59
Wing		Area in (m)
Wing area		1.02
Wing aspect ratio		6.25
Aerodynamic airfoil		CH10/FX63-137
Horizontal Tail(HT)		
HT area		.085
HT aspect ratio		3
HT aerodynamic airfoil		NACA0010
HT tail volume coefficient		0.229
Vertical Tail(VT)		
VT area		.0425
VT aspect ratio		2
VT aerodynamic		EPPLER EA(-1)012

Table2: Maximum Dimensions

The Figure 3, shows the geometrical model of unmanned aerial vehicle, the entire UAV model has been developed with the help of CATIA V5R20.

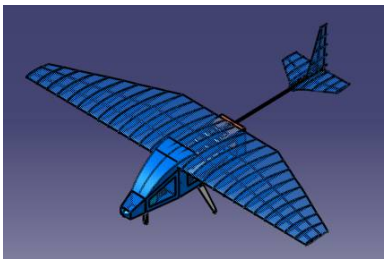

Fig 3: Full Assembly of the UAV CAD Model

3.2 FE Modeling

Modeling is a term that tends to be used for two distinct tasks in engineering. The objective in this approach is to identify the simplest model which can replicate the behaviour of interest. In this approach, model development is the process of identifying the ingredients of the model which can provide the qualitative and quantitative predictions. A second approach to modeling, which is becoming more common in industry, is to develop a detailed, single model of a design and to use it to examine all of the engineering criteria which are of interest. The impetus for this approach to modeling is that it costs far more to make a model or mesh for an engineering product than can be saved through reduction of the model by specializing it for each application. By using the same model for all of these analyses, a significant amount of engineering time can be saved. The finite element model may serve as a prototype that can be

ISSN(Online): 2319-8753
ISSN (Print): 2347-6710

International Journal of Innovative Research in Science, Engineering and Technology

(An ISO 3297: 2007 Certified Organization)

Vol. 5, Issue 6, June 2016

used for checking many aspects of a design's performance. The decreasing cost of computer time and the increasing speed of computers make this approach highly cost-effective.

3.2.1 Meshing In Hypermesh 9.0

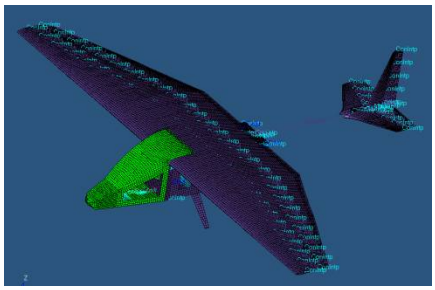

Fig4: Meshed model of the UAV

So Hypermesh (FEA Software) is a very effective application to prepare FE model of the UAV. This includes geometry clean up, mid surface extraction & shell meshing and The Project involved in generation of mid surface of the given component and is shell meshed with the required quality of the project.

Hence during meshing all surfaces are meshed using quad elements and some of the components like spars, pipes and connecting rod are assumed as beam and bar elements and most important components where our study is focused like fuel tank, receiver, battery, surveillance camera, servomotors, payload are assumed as mass elements concentrated at their centre of gravity.
Material properties are assigned to each type of elements based on their individual materials used for construction of the UAV. Cross sectional details are defined from basic geometry.
Elemental size for the UAV model is assumed to be 10mm as global size and based on that quality check has been done.

IV. SOLUTION METHOD- EXPLICIT TIME INTEGRATION

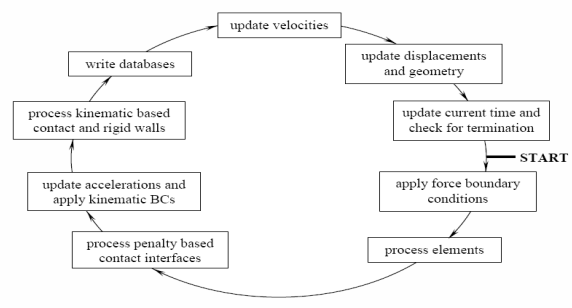

Fig5: Graphical description of explicit time integration

Explicit refers to the numerical method used to represent and solve the time derivatives in the momentum and energy equations. Fig 5 presents a graphical description of explicit time integration.

- The displacement of node n2 at time level $t+\Delta t$ is equal to known values of the displacement at nodes n1, n2, and n3 at time level t.
- A system of explicit algebraic equations is written for all the nodes in the mesh at time level $t+\Delta t$. Each equation is solved in-turn for the unknown node point displacements.
- Explicit methods are computational fast but are conditionally stable.
- The time step, Δt, must be less than a critical value or computational errors will grow resulting in a bad solution.

ISSN(Online): 2319-8753
ISSN (Print): 2347-6710

International Journal of Innovative Research in Science, Engineering and Technology

(An ISO 3297: 2007 Certified Organization)

Vol. 5, Issue 6, June 2016

- Explicit analysis solves using Central difference method

The time step must be less than the length of time it takes a signal travelling at the speed of sound in the material to traverse the distance between the node points.
In the central difference scheme, the velocities are approximated by

$$\dot{u}^n = v^{n+1/2} \equiv \frac{u^{n+1/2}}{\Delta t} - \frac{u^{n-1/2}}{\Delta t} = \frac{u(t+1/2) - u(t-1/2)}{\Delta t}$$

The value of the derivative at the centre of a time step is obtained from the difference of the function values at the ends of the time interval, hence the name central difference formula

4.1 Time Step Calculations for Shell Elements

For the shell elements, the time step size is given by

$$\Delta t_e = \frac{L_S}{c} \quad (4.5)$$

Where, $L_S$is the characteristic length and $C$is the sound speed

$$c = \sqrt{\frac{E}{\rho(1-V^2)}} \quad (4.6)$$

Three user options exist for choosing the characteristic length. In the default or first option the characteristic length is given by

$$L_s = \frac{(1+\beta)A_S}{\max(L_1, L_2, L_3, (1-\beta)L_4)} \quad (4.7)$$

Where β with algebraic coefficients β□ □0 for quadrilateral and 1 for triangular shell elements, A_S is the area, andLi, (i= 1 . . . . 4) is the length of the sides defining the shell elements. In the second option a more conservative value of $L\ s$ is used

$$L_s = \frac{(1+\beta)A_S}{\max(D_1, D_2)} \quad (4.8)$$

Where D_i (i=1, 2) is the length of the diagonals. The third option provides the largest time step size and is frequently used when triangular shell elements have very short altitudes.

$L_S$is given by, $L_s = max\left[\frac{(1+\beta)A_S}{\max(L_1, L_2, L_3, (1-\beta)L_4)}, \min(L_1, L_2, L_3, L_4 + \beta 10^{20})\right]$

4.2 Contact -Impact Problem in General

In crash simulation of airplanes, many components, including the engine, landing gears, etc., can contact during the crash and their surfaces are treated as sliding interfaces. The treatment of impact always requires a subsequent treatment of contact, since bodies which impact will stay in contact until rarefaction waves result in release. In the governing equations for bodies in contact kinetic and kinematic conditions on the contact interface are to be considered. The key condition is the condition of impenetrability: namely, the condition that two bodies cannot interpenetrate. The general condition of impenetrability cannot be expressed as a useful equation, so several approaches to developing specialized forms of these conditions have evolved.

Contact-impact problems are among the most difficult nonlinear problems because the response in contact-impact problems is not smooth. The velocities normal to the contact interface are discontinuous in time when impact occurs. When Coulomb friction models are used, the tangential velocities along the interface are discontinuous when stick-slip behaviour is encountered. These characteristics of contact-impact problems introduce significant difficulties in the time integration of the governing equations and impair the performance of numerical algorithms.

4.3 Fe Modeling of the UAV

In the present work, LS-DYNA is the chosen software and Crash analysis of a UAV has been done for two different configurations. LS-DYNA uses proven explicit time integration technique to solve the nonlinear dynamic response

ISSN(Online): 2319-8753
ISSN (Print): 2347-6710

International Journal of Innovative Research in Science, Engineering and Technology

(An ISO 3297: 2007 Certified Organization)

Vol. 5, Issue 6, June 2016

analysis problem. It contains a complete library of finite elements (type/shapes/orders) and numerous material models to simulate the nonlinear behaviour of materials.

4.3.1 Element Summary

Type Of Elements	Number of Elements
Shell, QUAD	40292
Shell, TRIA	538
Beam	116
Mass	6
Rbe3	107

Table 3: Element summary

4.4 Control Cards

These keyword cards are optional and can be used to change defaults, activate solution options such as Adaptive re-meshing, accuracy, hourglass, output etc. Control cards mainly used to control the some of the parameters during the solution process such that the simulation results will be of desired accuracy.

4.5 UAV Instrumentation Details

Sl. No.	Instruments	Mass (Kg)
1	Engine	0.55
2	Fuel tank	0.3
3	Batteries	0.119
4	Servo motors	0.07
5	Receiver	0.008
6	Payload	14

Table 4. Finite Elements used to model instruments [2] – as mass elements

4.6 Contact Types -Automatic Single Surface

Automatic single surface contact helps in defining the contact within structure and avoids penetration of the elements.

4.7 Control Termination

Set structural time step size control using different options.

- Time step is determined automatically (default)
- Constant time setep determined by the user (Paramter DT2MS).
- The mass is scaled for elements that violate the time step. The total duration chosen depends on the analysis.

4.8 Post Processing Options

Following are the post processing options used in LS-DYNA to obtain various plots and results**.**

4.9 Database Control

- database control is used for setting result output
- default is just the output of the *d3hsp* file, the protocol file (ascii)
- the result output is defined by the *database* cards.

ISSN(Online): 2319-8753
ISSN (Print): 2347-6710

International Journal of Innovative Research in Science, Engineering and Technology

(An ISO 3297: 2007 Certified Organization)

Vol. 5, Issue 6, June 2016

4.10 Database Binary D3plot

- Sets the frequency of the displacement, stress output, strains, velocities, accelerations etc.
- Writes the *d3plot* files (binary).

4.11 Database Nodal Force Group

The nodal reaction forces in the global or local X,Y and Z directions are printed in to the NODFOR ascii file along with the external work which is a result of these reaction forces.

V. RESULTS AND DISCUSSION

Crash analysis has been conducted on the UAV for two different configurations and posts processing of the results were done for both the configuration to determine force and energyplots.

5.1 Configuration - 1 Nose Down Collision

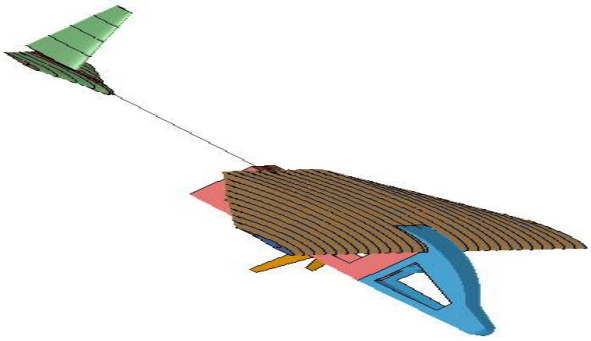

Fig 6: Nose down collision at t=0 sec

In the above Figure 6. The UAV just initiates impact at time 0.001 sec and there is not much damage seen in nose cone section.

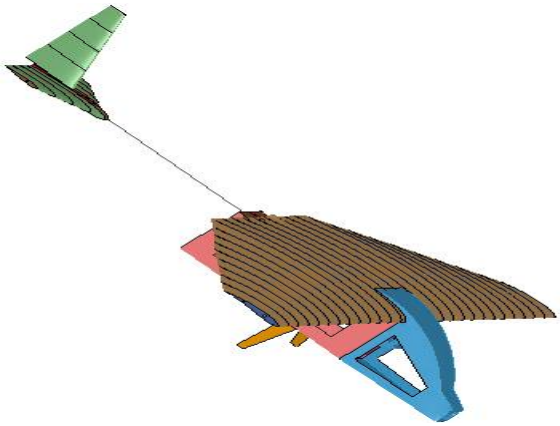

Fig 7: Nose down collision at t=0.003 sec

As time progresses, there is much damage in the nose cone section of UAV at time t=0.003 sec and most of the components are exposed to impact forces as shown in Figure 7.

ISSN(Online): 2319-8753
ISSN (Print): 2347-6710

International Journal of Innovative Research in Science, Engineering and Technology

(An ISO 3297: 2007 Certified Organization)

Vol. 5, Issue 6, June 2016

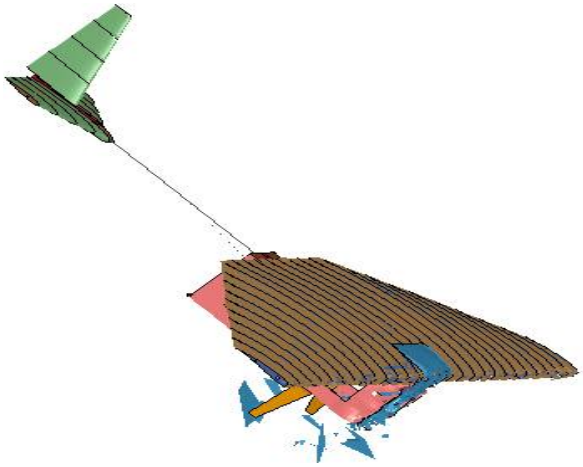

Fig 8: Nose down collision at t=0.007 sec

In Figure 8, all necessary components installed in the nosecone and fuselage are exposed to impact forces and all the components like receiver, battery, fuel tank, servomotor and payload have been collapsed at time t=0.007 sec. Analysis is now stopped.

5.2 Impact Forces

All the necessary equipment's in the UAV are modeled as mass elements and force time histories are captured for individual equipment to know the resultant forces acting on them**.**

Resultant forces on receiver and servo motor are captured over time and maximum resultant force is found to be 1.58e4N and 1.182e5N respectively. And on receiver and servo- motor, is found to be at time 5.64e-3 sec and 4.57e-3 seconds.

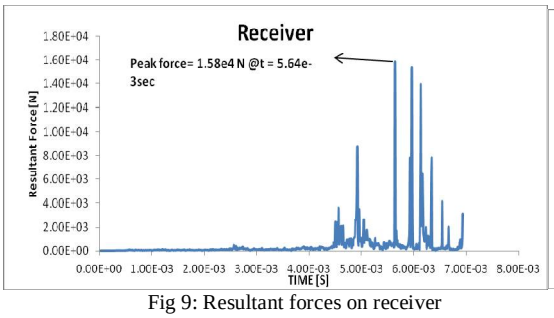

Fig 9: Resultant forces on receiver

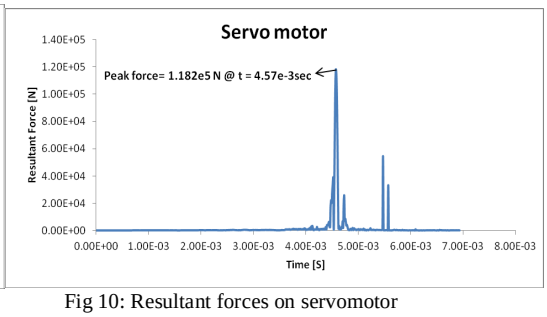

Fig 10: Resultant forces on servomotor

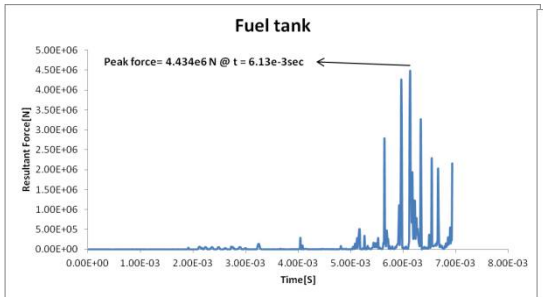

Fig 11: Resultant forces on fuel tank

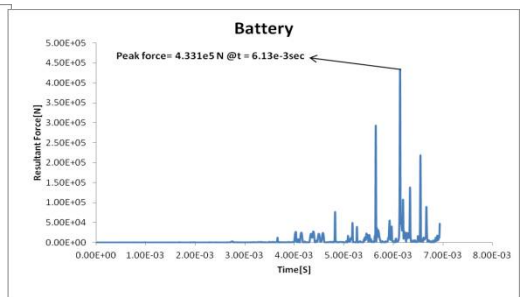

Fig 12: Resultant forces on battery

ISSN(Online): 2319-8753
ISSN (Print): 2347-6710

International Journal of Innovative Research in Science, Engineering and Technology

(An ISO 3297: 2007 Certified Organization)

Vol. 5, Issue 6, June 2016

The Figure 13 describes about resultant force on payload over time history is plotted in Figure 13 and maximum impact resultant force found on payload at time 6.87e-3 sec is 6.133e6N. So, the maximum impact resultant force is found in payload as well as in fuel tank when it is compared to other components of UAV.

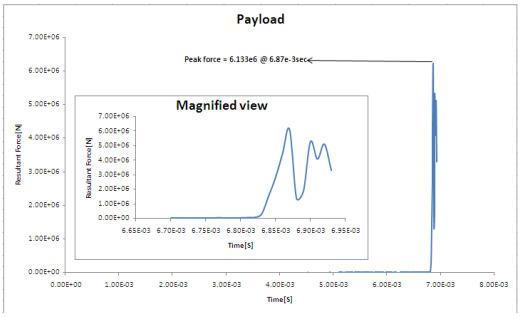

Fig 13: Resultant forces on payload

5.3 Maximum Principle Stress

The Figure 14 shows the maximum principle stresses during nose down collision at time t=0.00082 sec, the UAV experiences a maximum principle stress of 161891N in element number 2481 of the nosecone section as show in Figure 14.

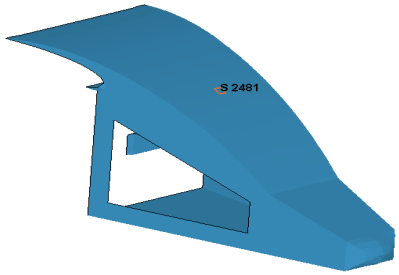

Fig 14: Nose cone model with maximum principle stress at element #2481

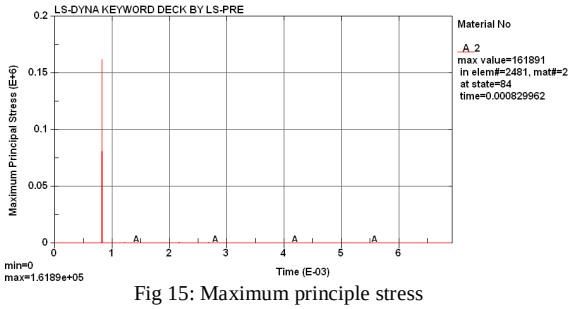

Fig 15: Maximum principle stress

5.4 Configuration -2 Belly Landing Collision

Landing gear experiences the most impact force in belly landing collision, but our focus is on the most important components like payload, batteries and engine etc.Figure 16 shows damages in the UAV structure at time t=0.003 seconds.

ISSN(Online): 2319-8753
ISSN (Print): 2347-6710

International Journal of Innovative Research in Science, Engineering and Technology

(An ISO 3297: 2007 Certified Organization)

Vol. 5, Issue 6, June 2016

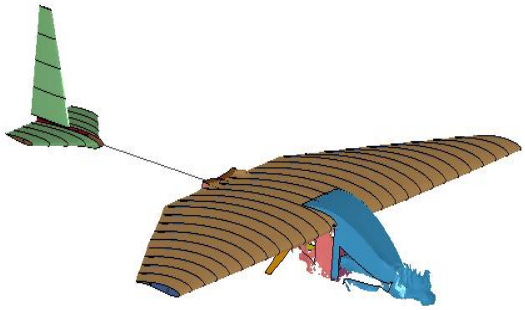

Fig 16: Belly landing collision at t=0.003sec

Landing gear experiences the most impact force in belly landing collision, but our focus is on the most important components as mentioned earlier and Figure 16. Shows damages in the UAV structure at time t=0.003 seconds.

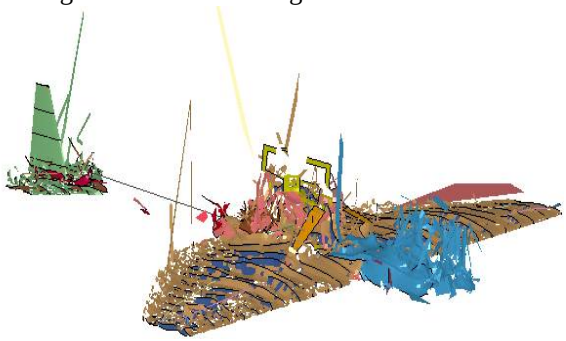

Fig 17: Belly landing collision at t=0.005sec

All the necessary components of UAV structure like receiver, servomotor, fuel tank, battery and payload are collapsed at time t=0.005 seconds and then analysis is stopped.

5.5 IMPACT FORCES

The Figure 18-19 shows the resultant forces on receiver and servo motor are captured over time and maximum resultant force is found to be 8.958e5N and 9.15e5N respectively at time 3.55e-3 sec and 2.65e-3 seconds.

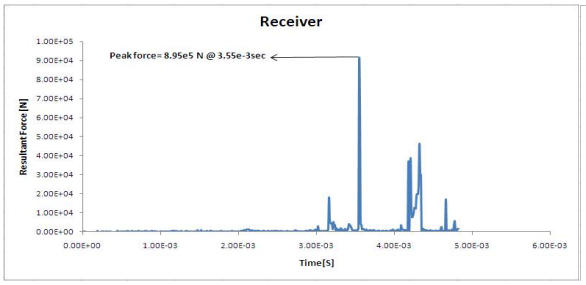

Fig 18: Resultant forces on receiver

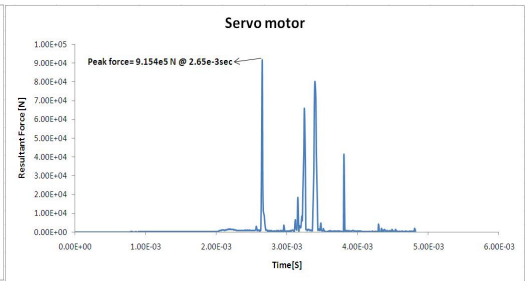

Fig 19: Resultant forces on servo motor

ISSN(Online): 2319-8753
ISSN (Print): 2347-6710

International Journal of Innovative Research in Science, Engineering and Technology

(An ISO 3297: 2007 Certified Organization)

Vol. 5, Issue 6, June 2016

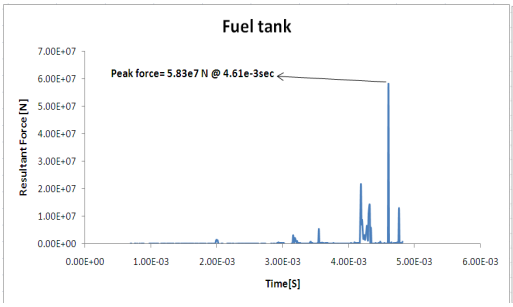

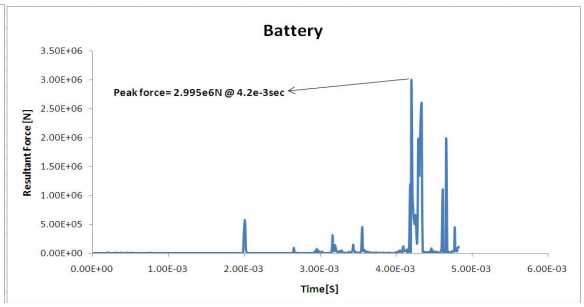

Fig 20: Resultant forces on fuel tankFig 21: Resultant forces on battery

The above Figure 20-21 shows the resultant impact forces are captured on fuel tank and battery over time history and peak impact forces are found to be 5.83e7N and 2.99e6N respectively at time 6.13e-3seconds and 4.2e-3 seconds.

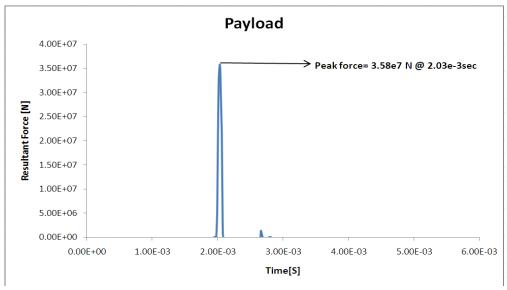

Fig 22: Resultant forces on payload

Figure 22 shows the maximum resultant force of 3.58e7N on payload at time t=2.03e-3 seconds is shown and from the Figure 20-22, it is noticed that both the fuel tank and payload experiences the maximum impact forces during belly landing collision.

5.6 MAXIMUM PRINCIPLE STRESS

The Figure 24 shows the maximum principle stress during belly landing collision at time t = 0.00437 sec, the UAV experiences a maximum principle stress of 43605N in element number 8914 of wing tip section.

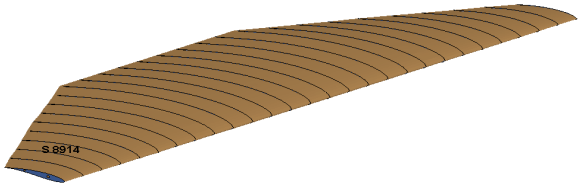

Fig 23: Maximum principle stress on element#8914

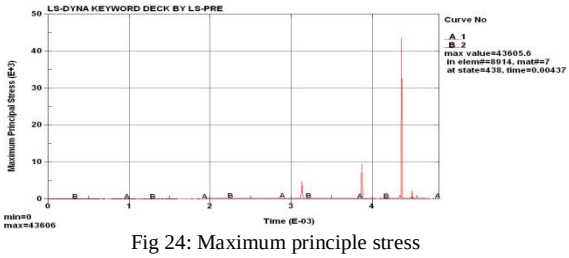

Fig 24: Maximum principle stress

ISSN(Online): 2319-8753
ISSN (Print): 2347-6710

International Journal of Innovative Research in Science, Engineering and Technology

(An ISO 3297: 2007 Certified Organization)

Vol. 5, Issue 6, June 2016

5.7 MATERIAL SUMMATION

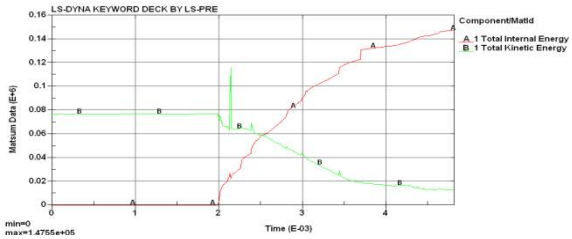

Fig 25: Material summation

Before crash, both total internal energy and total kinetic energy of the system remains constant. At crash the total kinetic energy reduces and total internal energy of system increases as shown in Figure 25.

VI. CONCLUSION

Crash analysis has been conducted on the UAV for two different configurations and posts processing of the results were done for both the configurations to determine force and energy plots.
All the necessary equipment's in the UAV are modeled as mass elements and force time histories are captured for individual equipment's to know the resultant force acting on them.

Sl. No.	COMPONENTS	PEAK IMPACT FORCE (N)	TIME (Sec)
1	Receiver	1.58e4	5.64e-3
2	servo motor	1.182e5	4.57e-3
3	fuel tank	4.434e6	6.13e-3
4	battery	4.331e5	6.13e-3
5	payload	6.133e6	6.87e-3

Table 5: Resultant forces on components in nose down collision

This analysis concludes that the components and supporting structure should be designed to overcome these peak forces in the particular location of UAV structure.
From the energy plot it assumed that internal energy and kinetic energy is almost remaining constant and during major impact the kinetic energy shows increase because of peak force acts in system during that time.
At time zero sec, the maximum principle stress is zero and when UAV touches or impacts it reaches up to a maximum value 161891 N at time 0.00082 sec in element number 2481 at the nose cone structure of UAV. So the present study is an attempt to find the peak impact forces acting on the important components of UAV during nose down collision.
Crash is a phenomenon which we can't avoid but we can reduce damages to the structural components. In this case, we should bring back the UAV in control and thereby we can reduce altitude as well as terminal velocity of the UAV which in-turn reduces resultant impact force.

ISSN(Online): 2319-8753
ISSN (Print): 2347-6710

International Journal of Innovative Research in Science, Engineering and Technology

(An ISO 3297: 2007 Certified Organization)

Vol. 5, Issue 6, June 2016

Sl. No.	COMPONENTS	PEAK IMPACT FORCE (N)	TIME (Sec)
1	Receiver	8.95e5	3.55e-3
2	servo motor	9.154e5	2.65e-3
3	fuel tank	5.83e7	4.61e-3
4	battery	2.995e6	4.2e-3
5	payload	3.58 e7	3.03e-3

Table 6: Resultant forces on components in belly landing collision

This analysis concludes that the components and supporting structure should be designed to overcome these peak forces in the particular location of UAV structure.
From the energy plot it assumed that internal energy and kinetic energy almost remain constant and during major impact the kinetic energy shows increase because of peak force acting during that time.
At time zero sec maximum principle stress is zero and when UAV touches or impacts, it reaches up to a maximum value of 43605 N at time 0.00437 sec in element number 8914 at the wing structure of UAV.
Before crash both total internal energy and total kinetic energy of system remains constant and when it crashes total kinetic energy reduces and total internal energy of system increases.
So the present study is an attempt to find peak forces acting on the important components of UAV during belly landing collision and based on the peak resultant force and maximum principle stress, we can go for the design of important components and its supporting structures.
In both the configuration collisions, belly landing collision experiences maximum resultant forces in the components like fuel tank and payload than the nose down collision of UAV. That can be overcome by placing impact shock absorbers or composite material as supporting structure.

Author Biography: Mr MAHANTAYYA K HIREMATH, a well-known Assistant Professor and researcher. He has mixed experienceof industry as well as teaching in the area of mechanical and aeronautical engineering. He has taughtvarious subjects like finite element methods, strength of materials, aircraft structures, flight vehicledesign, aircraft performance etc.

His area of research includes structural mechanics, Structural analysis and structural design and FEM andCFD.Author has been working on Design, development of Unmanned Aerial Vehicle for various applicationsin the field of agriculture, rescue operations, surveillance etc.

REFERENCES

[1] FENG Zhenyu, HAO Peng, ZOU Taichung. "Research Development of Crashworthiness Simulation Evaluation on Civil Aircraft" The 2nd International Symposium on Aircraft Airworthiness (ISAA 2011)
[2] Miguel Jimenez, Ricardo Andres Lugo, Carlos Daniel Rojas. "Sea Brazil Aero Design Challenge" FIU, 1 December 2011
[3] Martin S. Annett, "Analysis of Full Scale Helicopter Crash Test" 11th International LS DYNA Users Conference
[4] Karen E, Jackson, Edwin, "development of LS DYNA model of an ATR42-300 aircraft for crash simulation". 8th International LS DYNA Users Conference
[5] Marcio J. Cavalcanti, RadeVignjevic "A MSC/Dytran Simulation of The Lynx Helicopter Main Lift frame Collapse". Cranfield University, Cranfield, Bedford, United Kingdom
[6] Prof. G. Forasassi, Dr. R. Lo Frano, "Preliminary analysis of an aircraft impact", Cirten-UnipiRl 1059, Pisa, Giugno 2010
[7] A. B. PIFKO , R. WINTER, 'Theory And Application Of Finite Element Analysis To Structural Crash Simulation", Computers And Structures , Vol 13, PP 277-285 1981
[8] S Heimbs, F Strob, P Middendorf, J. M Guimard, "Composite crash absorber for aircraft fuselage applications", WIT Transactions on the Built Environment, Vol113, 2010
[9] M. J. Bayarri, James O. Berger, Marc C. Kennedy, AthanasiosKottas, Rui Paulo,
[10] Jerry Sacks, John A. Cafeo, Chin-Hsu Lin, and JianTu, "Predicting Vehicle Crashworthiness Validation of Computer Models for Functional and Hierarchical Data",National Institute of Statistical Sciences
[11] Anderson, David F.."Understanding Flight". New York, NY: McGraw-Hill, 2001
[12] Anderson, John. Fundamentals of Aerodynamics. McGraw Hill. New York, NY. 2001
[13] Chun-Yung Niu, Michael. "Airframe Structural Design": Practical Design Information and Data on Aircraft Structures. 2 ed. AdasoAdastra Engineering Center, 2006.
[14] Corke, Thomas. "Design of Aircraft". Prentice Hall: New Jersey, 2003.
[15] Nitin S Gokhale, Sanjay S Deshpande, Sanjeev V Bedekar,Anand N Thite, "Practical Finite Element Analysis" ,Finite To Infinite, Pune 2008